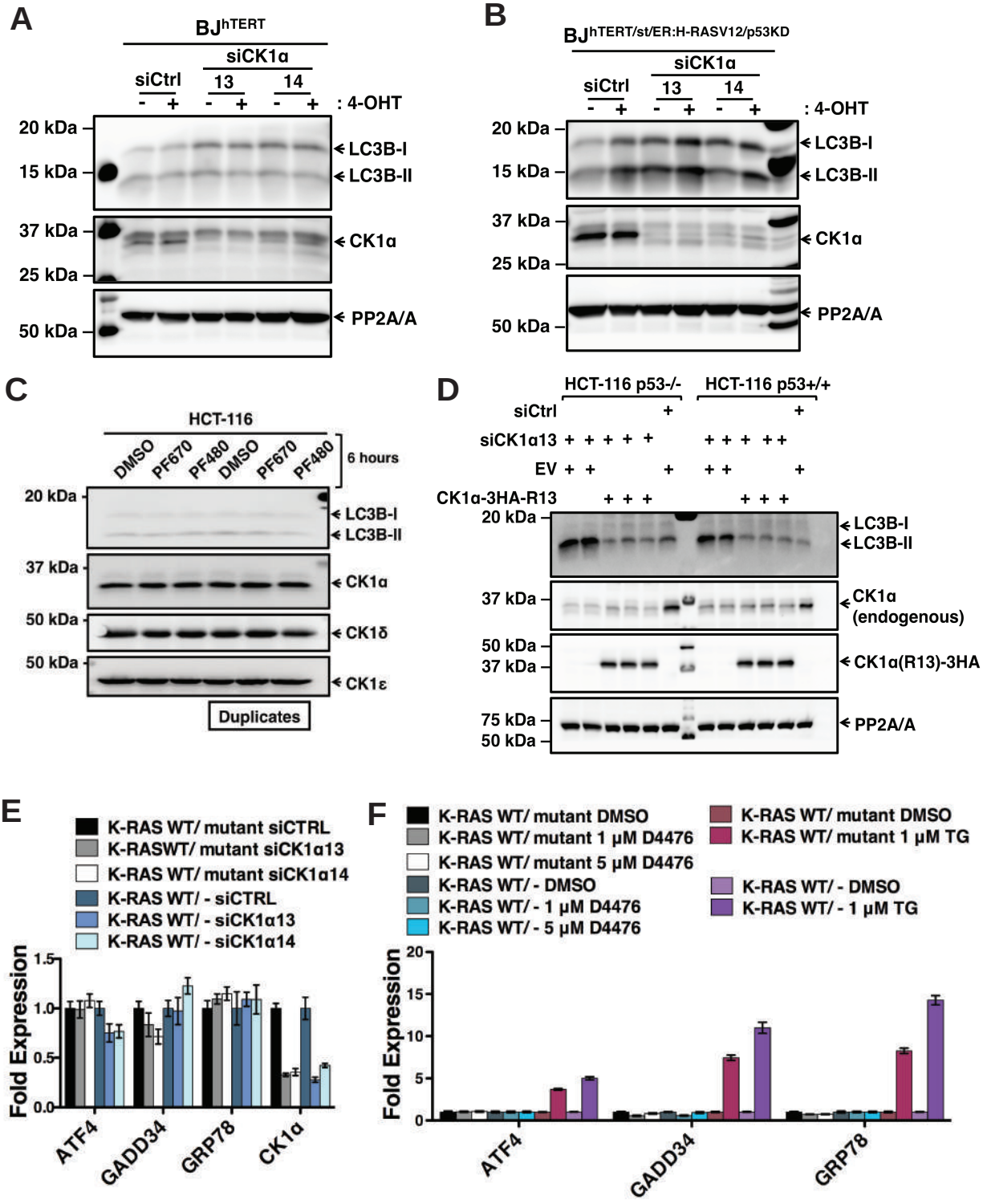

Supplemental Figure 1.
CK1α depletion or inactivation upregulates RAS-induced basal autophagy. (**A**) LC3B-II remains constant in CK1α-depleted BJ fibroblasts with wild-type RAS. BJ^{hTERT} fibroblasts were co-treated with siCtrl or siCK1α (#13 or #14), and 4-OHT (added 8 h post-RNAi transfection) for 72 h. (**B**) CK1α knockdown upregulates RAS-induced basal autophagy even when p53 is depleted. BJ$^{hTERT/st/ER:H-RASV12/p53KD}$ fibroblasts were co-treated with siCtrl or siCK1α (#13 or #14), and 4-OHT (added 8 h post-RNAi transfection) for 72 h. (**C**) Pharmacological inhibition of CK1δ or CK1ε fails to alter LC3B-II protein abundance. HCT-116 cells were exposed to DMSO, PF670 (1 μM) or PF480 (1 μM) for 6 h. (**D**) siRNA-resistant CK1α expression abolishes LC3B-II accumulation triggered by CK1α depletion. Isogenic HCT-116 cell lines (p53$^{-/-}$ and p53$^{+/+}$) were transfected with 0.5 μg pcDNA3.1 empty vector (EV) or pcDNA3.1-CK1α (R13)-3HA for 24 h, followed by transfection with siCtrl or siCK1α (#13 or #14) for an additional 48 h. (**E**) CK1α depletion or (**F**) inhibition by D4476 did not upregulate key ER stress factors (ATF4, GADD34 and GRP78) in isogenic HCT-116 lines (with/without mutant K-RAS), as assessed by qRT-PCR. 1 μM Thapsigargin (TG)-treated samples serve as positive control for ER stress induction. Cells were exposed to siCtrl, siCK1α (#13 or #14; for 48 h), or DMSO or 5 μM D4476 (for 6 h) prior to qRT-PCR analyses.

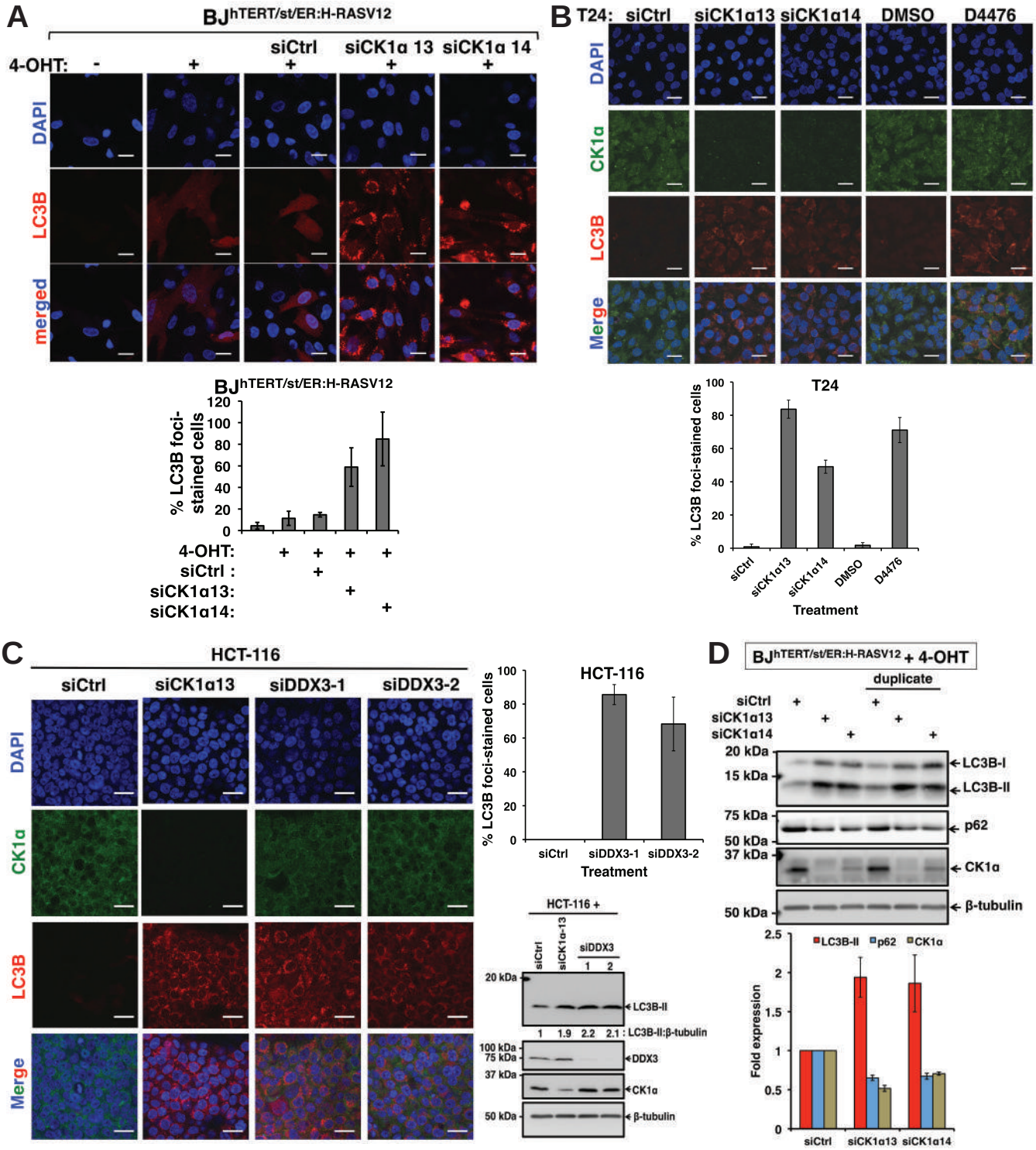

Supplemental Figure 2.
CK1α depletion or inactivation increases LC3B-II-associated autophagosomes in mutant RAS-driven cells. (**A**) CK1α depletion upregulates LC3B-II-associated autophagosomes. BJ$^{hTERT/st/ER:H-RASV12}$ fibroblasts were exposed to methanol or 4-OHT and the indicated siRNAs for 48 h. (**B**) CK1α depletion or inactivation upregulates LC3B-II-associated autophagosomes in T24 bladder cancer cells. Cells were exposed to the indicated siRNAs (for 48 h), DMSO or 5 μM D4476 (for 6 h). (**C**) DDX3 depletion upregulates LC3B-II-associated autophagosomes. HCT-116 cells were exposed to the indicated siRNAs for 48 h. Representative immunoblot of endogenous DDX3 and CK1α in these cells is included. Representative immunofluorescence images from three independent experiments are shown in **A**, **B** and **C**, where DAPI stains the nuclei. The associated bar charts represent LC3B foci-stained cells in each group that were quantified by the MetaMorph software (mean ± SD). Scale bar = 20 μm. (**D**) Protein abundance of LC3B-II and p62 is inversely correlated in CK1α depleted-BJ$^{hTERT/st/ER:H-RASV12}$ fibroblasts. Cells were analysed 48 h after transfection of the indicated siRNAs (in the presence of 4-OHT). The associated bar chart represents densitometric quantification of protein expression in Western blots from three independent experiments via the ImageJ software (mean ± SD).

Cheong et al. (Supplemental Figure 3)

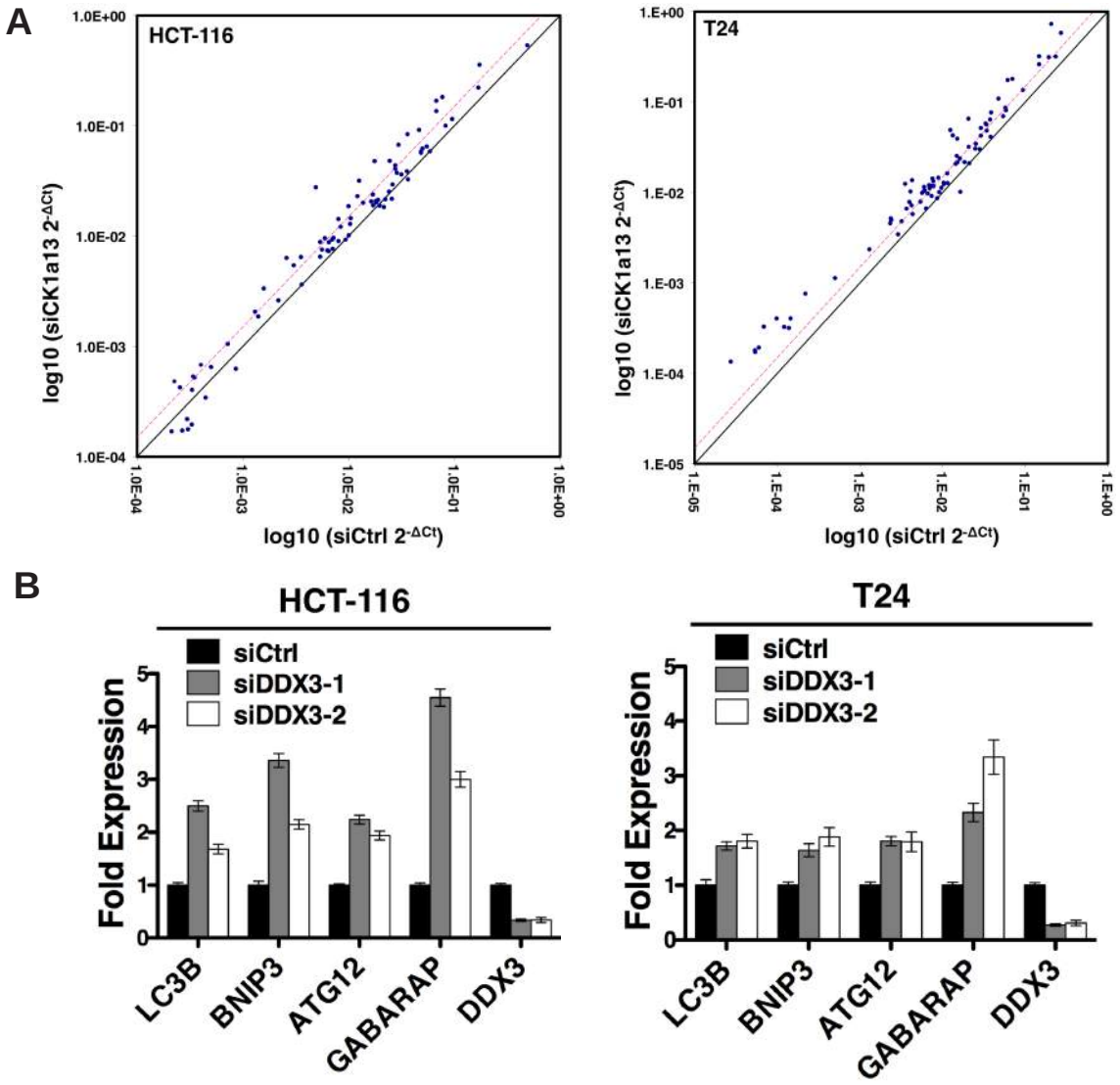

Supplemental Figure 3.
A FOXO3A autophagy gene transactivation signature upon CK1α depletion or inactivation. (**A**) RNAi depletion of CK1α dysregulates the expression of a subset of autophagy-related genes. Representative scatter plots of HCT-116 and T24 cancer cells treated with siCtrl or siCK1α (#13) for 24 h and probed for autophagy transcriptome changes via the Qiagen RT^2 Profiler^{TM} human autophagy real-time PCR arrays. (**B**) RNAi depletion of DDX3 upregulates a subset of FOXO3A-responsive autophagy-related genes. HCT-116 and T24 cancer cells are treated with siCtrl or siDDX3 (#1 or #2) for 48 h. Expression of FOXO3A-dependent autophagy genes in cell lysates are quantified using qPCR. Data are presented as fold-expression change relative to siCtrl. In **A**, each dot represents an individual autophagy-related gene. The bolded bar (in black) represents the mean, and the dashed bar (in pink) represents a 1.5-fold cut off. In **B**, β-actin and HPRT are used as normalizing controls. Data are presented as fold-expression change relative to respective controls. Data are mean ± SD of triplicate experiments.

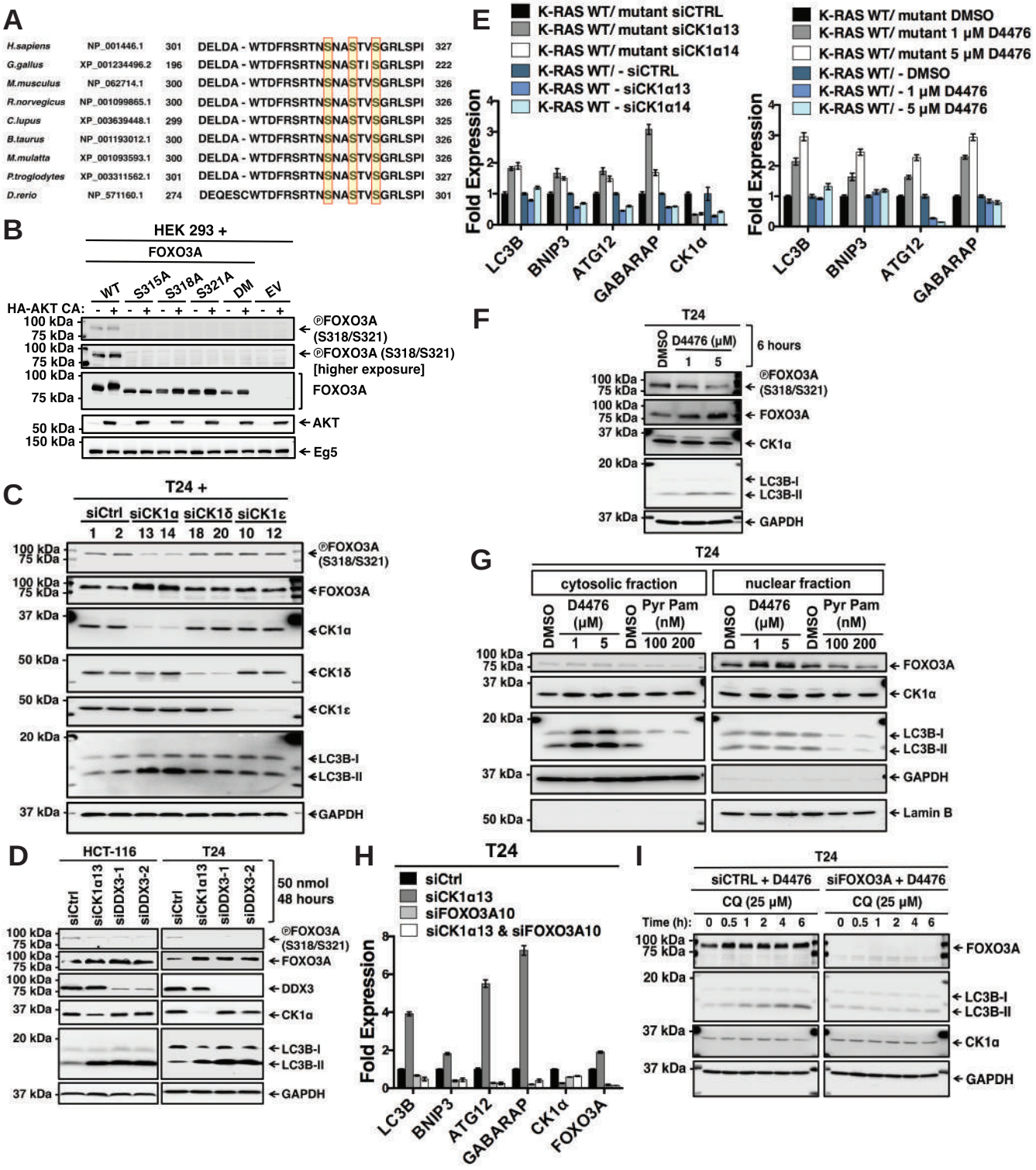

Supplemental Figure 4.
CK1α phosphorylates FOXO3A at S318 and S321, and regulates FOXO3A protein abundance in vivo. (**A**) The CK1α phosphorylation motif in FOXO3A is evolutionarily conserved. NCBI HomoloGene protein sequence alignment of FOXO3A across different species. (**B**) AKT-mediated phosphorylation of FOXO3A^{S315} further primes phosphorylation of FOXO3A$^{S318/321}$ by CK1α. HEK293 cells are co-transfected with wild-type (WT) or mutants of FOXO3A, together with either an empty vector (-) or a constitutively active HA-tagged AKT (+) for 72 h. Cell lysates were resolved by 8% SDS-PAGE. (**C**) CK1α is the only cytoplasmic CK1 isoform that phosphorylates FOXO3A in vivo. T24 cells are exposed to the indicated siRNAs for 48 h. (**D**) DDX3 depletion increases FOXO3A protein abundance by reducing phosphorylation of FOXO3A$^{S318/321}$. HCT116 and T24 cells are exposed to the indicated siRNAs for 48 h. (**E**) Upregulation of FOXO3A-responsive genes (*LC3B*, *BNIP3*, *ATG12* and *GABARAP*) upon CK1α depletion or inhibition is observed only in mutant Ras-driven cancer cells. Samples were assessed by qRT-PCR. β-actin and HPRT serve as normalizing controls. Data are presented as fold-expression change relative to respective controls. Data are mean ± SD of triplicate experiments. (**F**) D4476 dose-dependently reduces phosphorylation of FOXO3A$^{S318/321}$. T24 cells are exposed to the indicated drugs for 6 h. **(G)** Opposing effects of D4476 and Pyrvinium Pamoate (Pyr Pam) on the nuclear FOXO3A protein pool. T24 cells are exposed to the indicated drugs for 6 h**.** Lamin B and GAPDH serve as the loading control for nuclear and cytosolic fractions respectively. (**H**) CK1α requires FOXO3A to stimulate autophagy-related gene expression. Fold-expression changes of the indicated FOXO3A-dependent autophagy genes are determined by qPCR upon siCtrl, siCK1α (#13), siFOXO3A (#10), or both (siCK1α & siFOXO3A) in T24 cells. Data are mean ± SD of triplicate experiments. (**I**) CK1α inhibition-induced autophagic flux elevation in T24 cells requires FOXO3A. All data was derived from three independent experiments. Loading controls used in immunoblots include β-actin, GAPDH and Eg5.

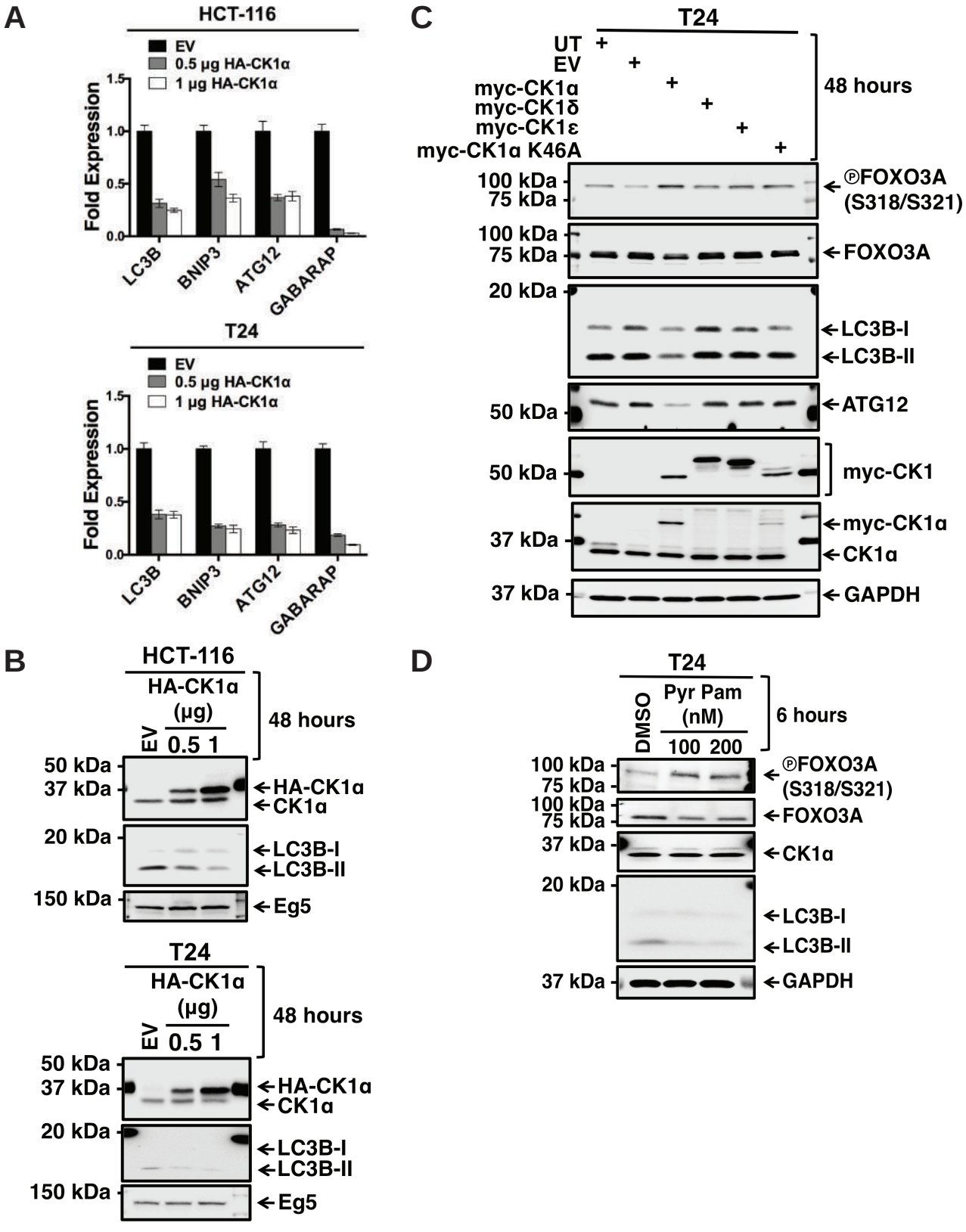

Supplemental Figure 5.
Overexpression or activation of CK1α suppresses FOXO3A-dependent autophagy-related gene transactivation by reducing FOXO3A protein abundance. (**A**) CK1α overexpression suppresses FOXO3A-dependent autophagy-related gene transactivation. HCT-116 and T24 are transfected with pCLneo (EV; 1 μg) or pCLneo-HA-CK1α (HA-CK1α; 0.5-1 μg) for 48 h. Expression levels of FOXO3A-dependent autophagy-related genes were quantified via qPCR. (**B**) Representative immunoblots of endogenous LC3B, CK1α and exogenous CK1α protein expression in cells from **A**. (**C**) Overexpression of catalytically active CK1α, not CK1δ or CK1ε, reduces FOXO3A and LC3B protein abundance. T24 cells are transfected with 1 μg EV, myc-CK1 isoforms and myc-CK1α K46A (kinase-dead) for 48 h. UT: untransfected. (**D**) Pyr Pam-induced activation of CK1α destabilizes FOXO3A by increasing FOXO3A$^{S318/321}$ phosphorylation. T24 cells are treated with DMSO or Pyr Pam (100 or 200 nM for 6 h). In **A**, β-actin and HPRT serve as normalizing controls. Data are mean ± SD of triplicate experiments and presented as fold-expression change relative to controls. All data was derived from three independent experiments. Loading controls used in immunoblots include Eg5 and GAPDH.

Cheong et al. (Supplemental Figure 6)

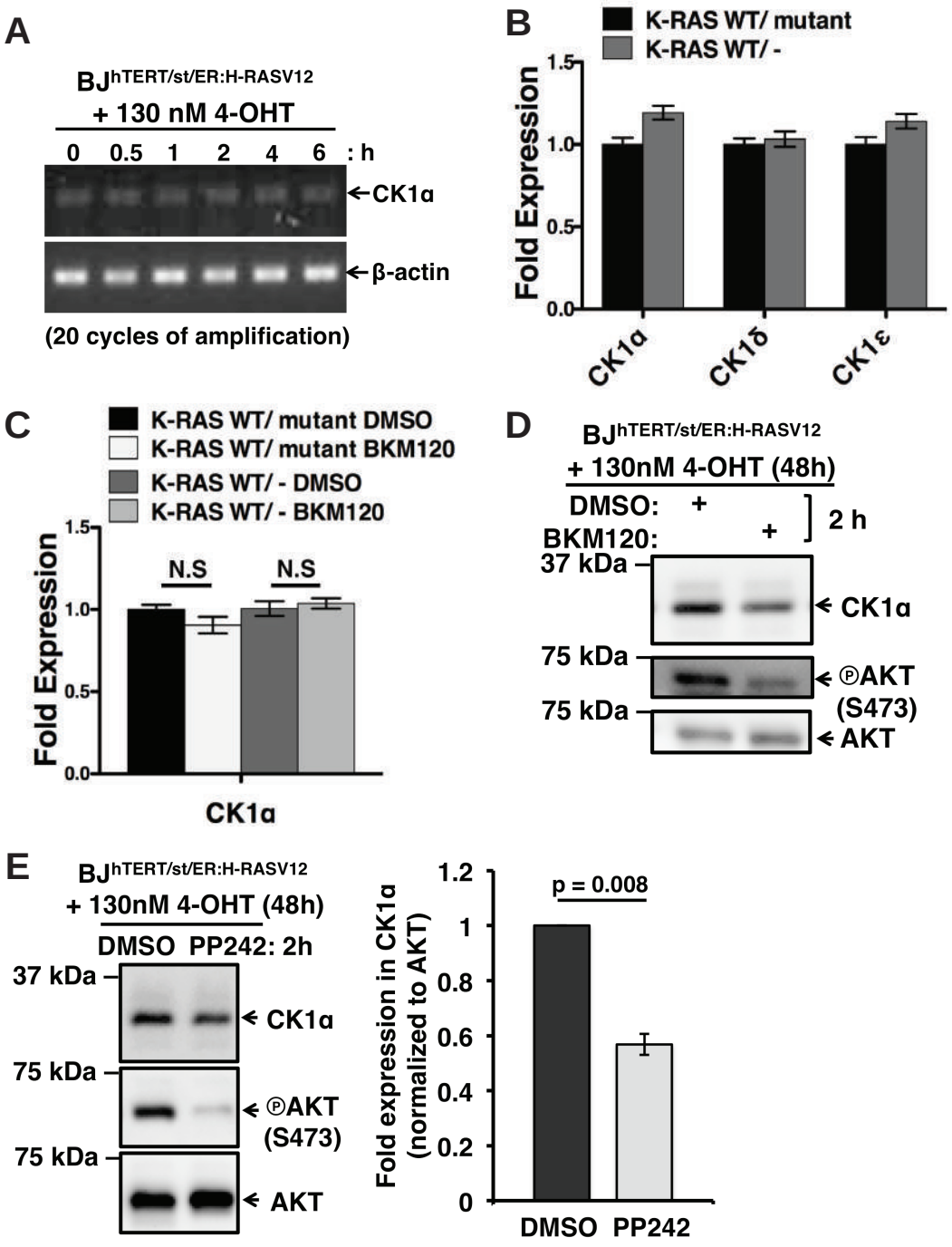

Supplemental Figure 6.
The PI3K-mTOR signaling axis regulates CK1α protein abundance in mutant RAS-driven cells. (**A**) CK1α transcript abundance remains constant upon oncogenic H-RAS^{V12} activation. Representative agarose gel image of CK1α transcript expression in BJ$^{hTERT/st/ER:H-RASV12}$ fibroblasts exposed to 4-OHT over the indicated time via semi-quantitative RT-PCR. (**B**) Transcript abundance of cytosolic CK1 isoforms remains constant regardless of mutant K-RAS status. qPCR profiling of CK1 isoform transcript expression in isogenic HCT-116 cells with or without mutant K-RAS. (**C**) CK1α transcripts remain constant regardless of class I PI3 kinase inhibition. CK1α transcript expression in isogenic HCT-116 cells (with or without mutant K-RAS) treated by DMSO or 0.5 μM BKM120 (class I PI3K inhibitor) was assessed by qRT-PCR. (**D**) PI3K inhibition reduces CK1α protein abundance. Representative immunoblot of endogenous CK1α protein expression in BJ$^{hTERT/st/ER:H-RASV12}$ fibroblasts exposed to 4-OHT for 48 h. 46 h post-4-OHT treatment, vehicle control (DMSO) or BKM120 (0.5 μM) is added to these cells for a further 2 h incubation prior to analysis. (**E**) Blockade of mTOR activity by PP242 reduces CK1α protein abundance. Representative immunoblot of endogenous CK1α protein expression in BJ$^{hTERT/st/ER:H-RASV12}$ fibroblasts exposed to 4-OHT for 48 h. 46 h post-4-OHT treatment, vehicle control (DMSO) or PP242 (0.2 μM) is added to these cells for a further 2 h incubation prior to analysis. Intensities of protein bands are quantified by densitometry (ImageJ). Fold-expression change in CK1α is first normalized to total AKT and then calculated relative to their treatment controls. All data was derived from three independent experiments. In **A**,**B** and **C**, β-actin serves as the loading control. In **D** and **E**, AKT serves as the loading control.

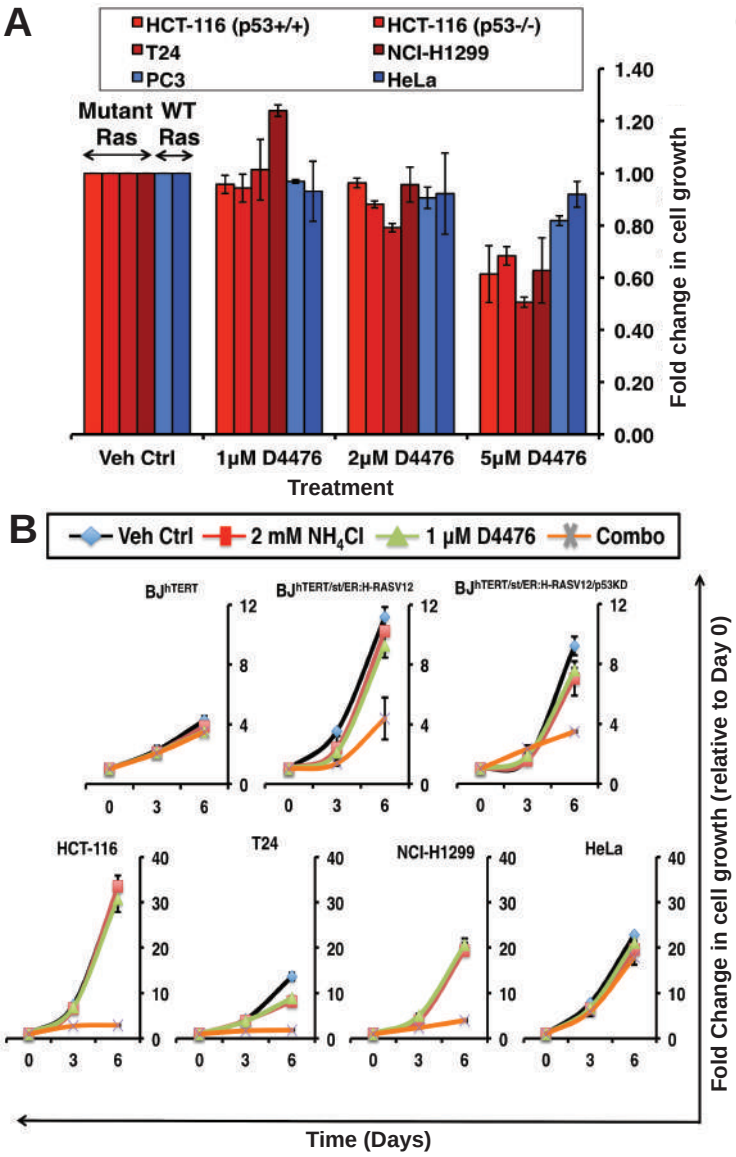

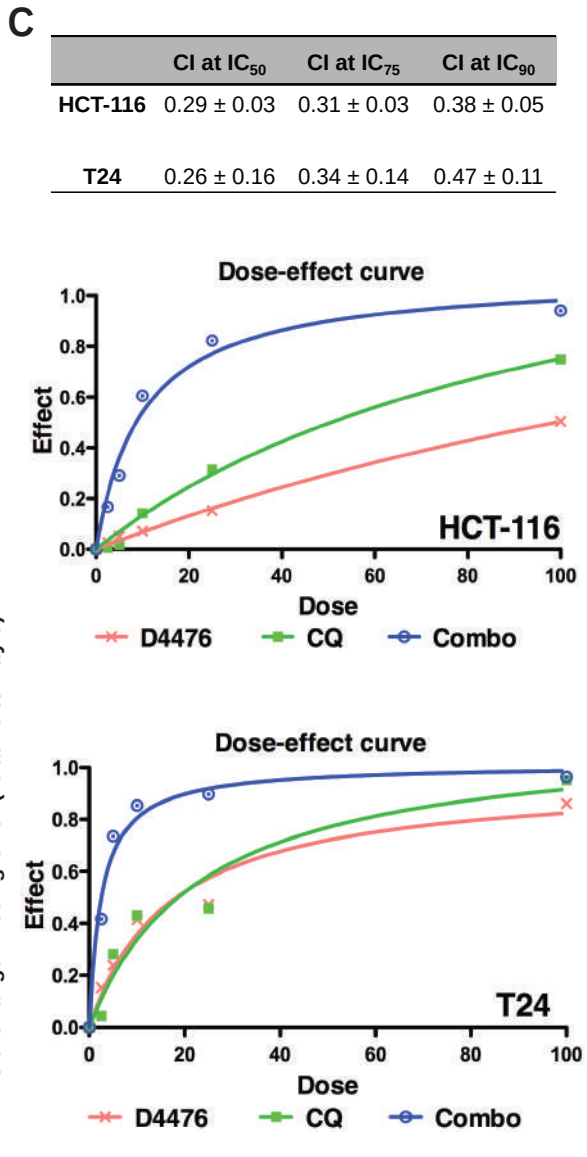

	CI at IC_{50}	CI at IC_{75}	CI at IC_{90}
HCT-116	0.29 ± 0.03	0.31 ± 0.03	0.38 ± 0.05
T24	0.26 ± 0.16	0.34 ± 0.14	0.47 ± 0.11

Supplemental Figure 7.
Synergistic interaction of CK1α and lysosomal inhibition induces growth arrest of RAS-driven human cancer cells. (**A**) D4476 modestly inhibits growth of human cancer cells driven by mutant RAS in a dose-dependent manner. A panel of human cancer cell lines that possess mutant RAS [in shades of red; HCT-116 ($p53^{-/-}$ and $p53^{+/+}$), T24 and NCI-H1299] or wild-type RAS [in shades of blue; PC3 and HeLa] are treated with Veh Ctrl (DMSO) or D4476 over 5 days, prior to methanol fixation, crystal violet staining and dye release for OD_{595} quantification. (**B**) Oncogenic RAS-driven cancer cells are sensitive to NH_4Cl:D4476 drug combination treatment. BJ-derived fibroblasts, HCT-116, T24, NCI-H1299 and HeLa cells are treated with vehicle control (Veh Ctrl; H_2O:DMSO), NH_4Cl, D4476 or drug Combo (NH_4Cl:D4476) over the indicated time, prior to methanol fixation, crystal violet staining and dye release for OD_{595} quantification. Fold change in transformed/cancer cell growth in **A** and **B** is calculated relative to growth prior to drug addition (Day 0). (**C**) D4476:CQ combination is synergistic. Combination indices (CI) at various growth inhibition rates (50%, 75% and 90%; Data are mean ± SD of triplicate experiments) and drug dose-effect curves were calculated the Calcusyn software. CI<1: synergistic; CI=1: additive; CI>1: antagonistic.

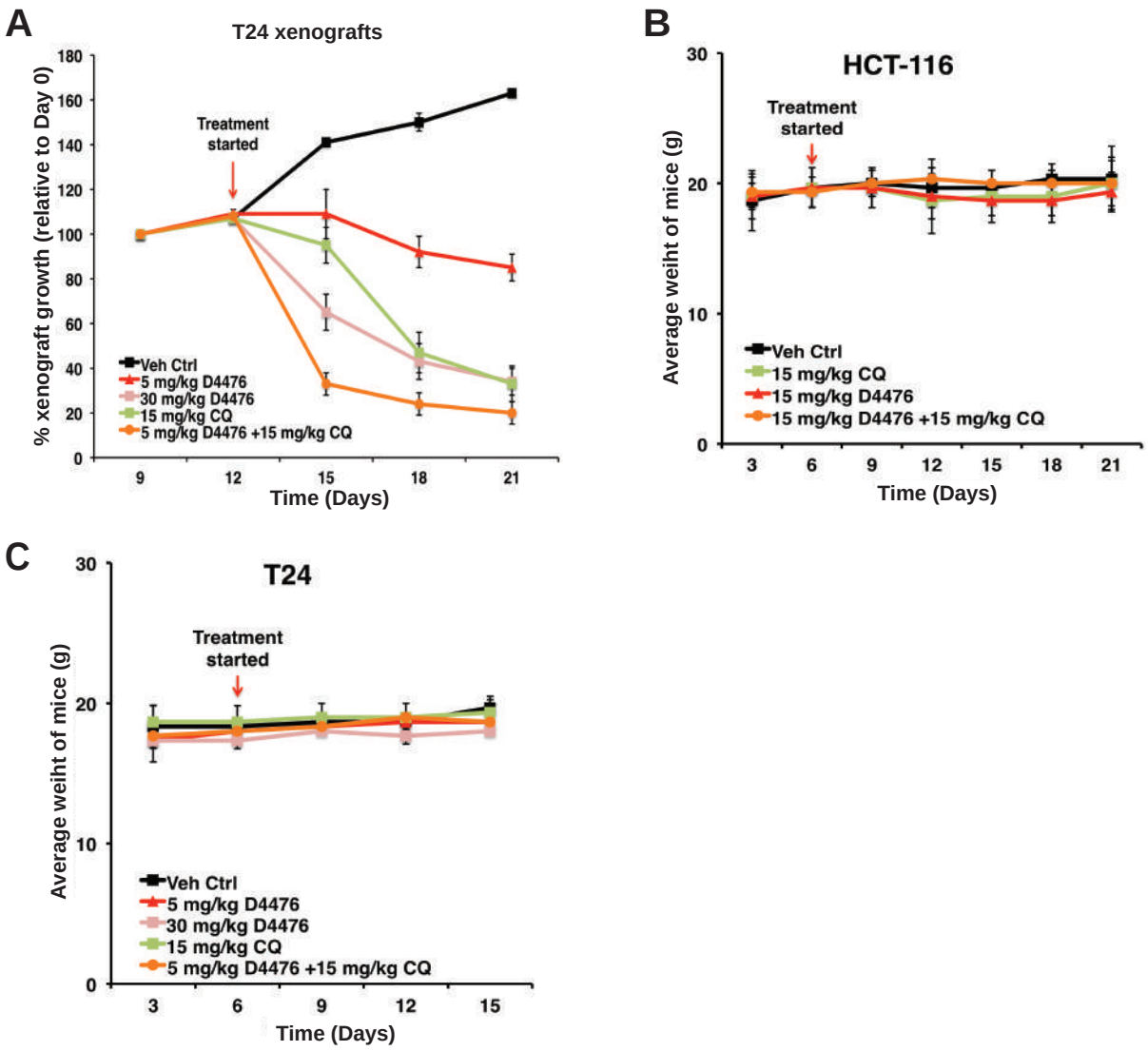

Supplemental Figure 8.
Synergistic interaction of CK1α and lysosomal inhibition induces growth arrest of RAS-driven tumor xenografts in mice. (**A**) CQ:D4476 drug combination treatment regresses growth of T24 tumor xenografts. BALB/C athymic nude mice with T24 tumor xenografts are intraperitoneally injected with Veh Ctrl, D4476, CQ or drug Combo (D4476 + CQ) over the indicated time (n = 3 mice in each treatment group, xenografts established at both flanks per mouse). % increase in xenograft growth is a measure of tumor ellipsoid volumes at time points after the commencement of drug treatment (from Day 12) relative to the last treatment naïve time point (Day 9). (**B**) CQ:D4476 drug combination treatment is not toxic to HCT-116 tumor xenograft- and (**C**) T24 tumor xenograft-bearing athymic nude mice. Body weight of BALB/C athymic nude mice with HCT-116 tumor xenografts (n = 6 mice in each group) are measured before and during the course of drug treatment; expressed as mean ± SD. Body weight of BALB/C athymic nude mice with T24 tumor xenografts (n = 3 mice in each group) are measured before and during the course of drug treatment; expressed as mean ± SD.

Cheong et al. (Supplemental Table 1)

Supplemental Table 1.
Expression of autophagy-related genes in oncogenic RAS-driven HCT-116 colon carcinoma after CK1α knockdown. Experiments are performed in triplicates.

Gene	AVG ΔC_t (Ct(GOI) - Ave Ct (HKG))		$2^{-\Delta C_t}$		Fold Change
	siCK1α13	siCtrl	siCK1α13	siCtrl	siCK1α13 / siCtrl
AKT1	4.94	4.78	3.3E-02	3.6E-02	0.89
AMBRA1	7.30	8.60	6.4E-03	2.6E-03	2.46
APP	2.17	2.57	2.2E-01	1.7E-01	1.32
ATG10	11.28	11.56	4.0E-04	3.3E-04	1.22
ATG12	3.44	4.44	9.2E-02	4.6E-02	1.99
ATG16L1	6.74	7.17	9.3E-03	6.9E-03	1.34
ATG16L2	8.22	9.30	3.4E-03	1.6E-03	2.12
ATG3	4.09	4.09	5.9E-02	5.9E-02	1.00
ATG4A	7.26	7.54	6.5E-03	5.4E-03	1.21
ATG4B	6.13	6.96	1.4E-02	8.0E-03	1.78
ATG4C	6.28	6.59	1.3E-02	1.0E-02	1.25
ATG4D	6.69	7.12	9.7E-03	7.2E-03	1.34
ATG5	5.72	5.67	1.9E-02	2.0E-02	0.96
ATG7	8.10	8.12	3.7E-03	3.6E-03	1.01
ATG9A	6.79	7.92	9.0E-03	4.1E-03	2.19
ATG9B	11.02	12.11	4.8E-04	2.3E-04	2.13
BAD	6.75	6.74	9.3E-03	9.4E-03	0.99
BAK1	7.05	7.48	7.5E-03	5.6E-03	1.34
BAX	4.51	5.17	4.4E-02	2.8E-02	1.58
BCL2	10.58	10.96	6.5E-04	5.0E-04	1.30
BCL2L1	4.37	5.36	4.8E-02	2.4E-02	1.98
BECN1	5.39	5.88	2.4E-02	1.7E-02	1.41
BID	3.12	3.39	1.1E-01	9.5E-02	1.21
BNIP3	2.57	3.89	1.7E-01	6.7E-02	2.50
CASP3	6.62	6.64	1.0E-02	1.0E-02	1.01
CASP8	7.08	7.31	7.4E-03	6.3E-03	1.17
CDKN1B	5.54	5.49	2.2E-02	2.2E-02	0.97
CDKN2A	5.77	5.54	1.8E-02	2.2E-02	0.85
CLN3	6.79	6.97	9.0E-03	8.0E-03	1.13
CTSB	5.09	5.27	2.9E-02	2.6E-02	1.13
CTSD	4.73	5.13	3.8E-02	2.9E-02	1.32
CTSS	10.91	11.48	5.2E-04	3.5E-04	1.49
CXCR4	10.64	10.19	6.3E-04	8.6E-04	0.73
DAPK1	10.52	11.28	6.8E-04	4.0E-04	1.70
DRAM1	5.74	6.65	1.9E-02	1.0E-02	1.87
DRAM2	3.89	5.07	6.7E-02	3.0E-02	2.26
EIF2AK3	6.82	7.26	8.8E-03	6.5E-03	1.36
EIF4G1	4.09	4.37	5.9E-02	4.8E-02	1.22
ESR1	12.50	11.86	1.7E-04	2.7E-04	0.65
FADD	5.64	6.19	2.0E-02	1.4E-02	1.46

Cell line: HCT-116 colon cancer cells

Cheong et al. (Supplemental Table 1)

Supplemental Table 1.
Expression of autophagy-related genes in oncogenic RAS-driven HCT-116 colon carcinoma after CK1α knockdown. Experiments are performed in triplicates.

FAS	5.58	5.79	2.1E-02	1.8E-02	1.15
GAA	4.38	5.83	4.8E-02	1.8E-02	2.72
GABARAP	2.88	3.89	1.4E-01	6.8E-02	2.01
GABARAPL1	4.97	6.32	3.2E-02	1.3E-02	2.53
GABARAPL2	2.46	3.70	1.8E-01	7.7E-02	2.36
HDAC1	3.31	3.60	1.0E-01	8.3E-02	1.22
HDAC6	6.71	7.39	9.6E-03	6.0E-03	1.60
HGS	6.11	6.58	1.5E-02	1.0E-02	1.39
HSP90AA1	0.01	-0.63	9.9E-01	1.5E+00	0.64
HSPA8	0.90	1.03	5.4E-01	4.9E-01	1.09
HTT	7.28	8.14	6.4E-03	3.5E-03	1.82
IFNG	13.31	12.29	9.9E-05	2.0E-04	0.49
IGF1	12.15	11.71	2.2E-04	3.0E-04	0.74
INS	14.03	13.40	6.0E-05	9.3E-05	0.64
IRGM	12.52	12.21	1.7E-04	2.1E-04	0.80
LAMP1	4.00	4.32	6.2E-02	5.0E-02	1.25
MAP1LC3A	11.20	11.94	4.3E-04	2.5E-04	1.67
MAP1LC3B	3.58	4.79	8.4E-02	3.6E-02	2.32
MAPK14	6.36	6.89	1.2E-02	8.4E-03	1.45
MAPK8	5.55	5.71	2.1E-02	1.9E-02	1.12
MTOR	5.30	5.37	2.5E-02	2.4E-02	1.05
NFKB1	7.02	7.15	7.7E-03	7.1E-03	1.09
NPC1	5.59	5.94	2.1E-02	1.6E-02	1.27
PIK3C3	5.63	5.78	2.0E-02	1.8E-02	1.11
PIK3CG	12.31	11.57	2.0E-04	3.3E-04	0.60
PIK3R4	5.72	5.88	1.9E-02	1.7E-02	1.12
PRKAA1	4.69	4.82	3.9E-02	3.5E-02	1.09
PTEN	4.62	5.17	4.1E-02	2.8E-02	1.47
RAB24	9.89	10.44	1.1E-03	7.2E-04	1.47
RB1	5.52	5.29	2.2E-02	2.6E-02	0.85
RGS19	6.82	7.54	8.9E-03	5.4E-03	1.65
RPS6KB1	4.13	4.37	5.7E-02	4.8E-02	1.18
SNCA	8.92	9.58	2.1E-03	1.3E-03	1.58
SQSTM1	1.48	2.53	3.6E-01	1.7E-01	2.07
TGFB1	4.79	4.99	3.6E-02	3.2E-02	1.15
TGM2	5.17	7.67	2.8E-02	4.9E-03	5.64
TMEM74	11.51	11.13	3.4E-04	4.5E-04	0.77
TNF	12.46	11.69	1.8E-04	3.0E-04	0.59
TNFSF10	10.87	11.53	5.4E-04	3.4E-04	1.58
TP53	3.94	4.19	6.5E-02	5.5E-02	1.19
ULK1	9.06	9.48	1.9E-03	1.4E-03	1.34
ULK2	7.52	8.37	5.4E-03	3.0E-03	1.80
UVRAG	8.58	8.85	2.6E-03	2.2E-03	1.20
WIPI1	5.44	6.37	2.3E-02	1.2E-02	1.90

Cell line: HCT-116 colon cancer cells

Cheong et al. (Supplemental Table 2)

Supplemental Table 2.
Expression of autophagy-related genes in oncogenic RAS-driven T24 bladder carcinoma cells after CK1α knockdown. Experiments are performed in triplicates.

Gene	AVG ΔC_t (Ct(GOI) - Ave Ct (HKG))		$2^{-\Delta C_t}$		Fold Change
	siCK1α13	siCtrl	siCK1α13	siCtrl	siCK1α13 / siCtrl
AKT1	4.15	4.88	5.6E-02	3.4E-02	1.66
AMBRA1	6.61	7.95	1.0E-02	4.1E-03	2.53
APP	1.65	2.10	3.2E-01	2.3E-01	1.37
ATG10	11.62	12.83	3.2E-04	1.4E-04	2.30
ATG12	4.55	6.23	4.3E-02	1.3E-02	3.21
ATG16L1	6.99	7.99	7.9E-03	3.9E-03	1.99
ATG16L2	6.59	7.40	1.0E-02	5.9E-03	1.75
ATG3	4.36	4.87	4.9E-02	3.4E-02	1.42
ATG4A	7.65	8.70	5.0E-03	2.4E-03	2.08
ATG4B	6.49	7.17	1.1E-02	6.9E-03	1.61
ATG4C	6.98	7.53	7.9E-03	5.4E-03	1.46
ATG4D	7.59	8.73	5.2E-03	2.4E-03	2.20
ATG5	6.10	6.82	1.5E-02	8.8E-03	1.65
ATG7	6.66	7.47	9.9E-03	5.6E-03	1.76
ATG9A	6.41	7.00	1.2E-02	7.8E-03	1.51
ATG9B	11.57	13.84	3.3E-04	6.8E-05	4.80
BAD	5.40	5.96	2.4E-02	1.6E-02	1.48
BAK1	6.38	7.19	1.2E-02	6.9E-03	1.75
BAX	4.55	5.11	4.3E-02	2.9E-02	1.47
BCL2	9.79	10.97	1.1E-03	5.0E-04	2.27
BCL2L1	4.11	4.92	5.8E-02	3.3E-02	1.75
BECN1	5.94	6.46	1.6E-02	1.1E-02	1.44
BID	3.96	4.74	6.4E-02	3.7E-02	1.72
BNIP3	1.64	2.77	3.2E-01	1.5E-01	2.19
CASP3	5.30	6.08	2.5E-02	1.5E-02	1.71
CASP8	6.78	7.08	9.1E-03	7.4E-03	1.24
CDKN1B	4.97	5.60	3.2E-02	2.1E-02	1.54
CDKN2A	4.28	5.11	5.2E-02	2.9E-02	1.78
CLN3	6.44	7.39	1.2E-02	6.0E-03	1.94
CTSB	3.70	4.69	7.7E-02	3.9E-02	1.99
CTSD	2.47	3.84	1.8E-01	7.0E-02	2.59
CTSS	6.33	8.15	1.2E-02	3.5E-03	3.53
CXCR4	8.18	8.43	3.5E-03	2.9E-03	1.19
DAPK1	12.34	14.03	1.9E-04	6.0E-05	3.23
DRAM1	5.53	6.04	2.2E-02	1.5E-02	1.43
DRAM2	5.54	6.06	2.1E-02	1.5E-02	1.44
EIF2AK3	7.12	7.89	7.2E-03	4.2E-03	1.71
EIF4G1	3.53	4.12	8.7E-02	5.8E-02	1.51
ESR1	11.27	13.32	4.1E-04	9.8E-05	4.14
FADD	4.85	5.32	3.5E-02	2.5E-02	1.38

Cell line: T24 bladder cancer cells

Supplemental Table 2.
Expression of autophagy-related genes in oncogenic RAS-driven T24 bladder carcinoma cells after CK1α knockdown. Experiments are performed in triplicates.

FAS	5.03	5.33	3.1E-02	2.5E-02	1.24
GAA	6.68	7.24	9.8E-03	6.6E-03	1.48
GABARAP	2.52	4.03	1.7E-01	6.1E-02	2.86
GABARAPL1	3.93	5.60	6.6E-02	2.1E-02	3.20
GABARAPL2	3.20	4.40	1.1E-01	4.7E-02	2.30
HDAC1	3.84	4.22	7.0E-02	5.4E-02	1.30
HDAC6	6.40	7.11	1.2E-02	7.2E-03	1.64
HGS	6.56	7.37	1.1E-02	6.0E-03	1.75
HSP90AA1	1.67	2.38	3.1E-01	1.9E-01	1.64
HSPA8	0.78	1.89	5.8E-01	2.7E-01	2.16
HTT	6.13	7.05	1.4E-02	7.5E-03	1.90
IFNG	12.50	14.19	1.7E-04	5.4E-05	3.21
IGF1	11.58	13.01	3.3E-04	1.2E-04	2.70
INS	12.85	15.16	1.4E-04	2.7E-05	4.96
IRGM	12.44	14.19	1.8E-04	5.3E-05	3.37
LAMP1	3.62	4.10	8.1E-02	5.8E-02	1.40
MAP1LC3A	6.19	7.88	1.4E-02	4.3E-03	3.22
MAP1LC3B	4.67	6.05	3.9E-02	1.5E-02	2.61
MAPK14	6.86	6.86	8.6E-03	8.6E-03	1.00
MAPK8	6.47	6.70	1.1E-02	9.6E-03	1.17
MTOR	5.59	6.13	2.1E-02	1.4E-02	1.45
NFKB1	6.34	6.59	1.2E-02	1.0E-02	1.19
NPC1	4.34	6.34	4.9E-02	1.2E-02	3.99
PIK3C3	6.29	6.45	1.3E-02	1.1E-02	1.11
PIK3CG	10.36	12.16	7.6E-04	2.2E-04	3.49
PIK3R4	6.62	6.79	1.0E-02	9.0E-03	1.12
PRKAA1	4.59	4.72	4.1E-02	3.8E-02	1.09
PTEN	5.56	5.57	2.1E-02	2.1E-02	1.01
RAB24	8.73	9.59	2.4E-03	1.3E-03	1.82
RB1	5.05	5.15	3.0E-02	2.8E-02	1.07
RGS19	6.23	7.02	1.3E-02	7.7E-03	1.72
RPS6KB1	5.53	5.77	2.2E-02	1.8E-02	1.18
SNCA	7.66	8.72	5.0E-03	2.4E-03	2.09
SQSTM1	0.45	2.29	7.3E-01	2.0E-01	3.57
TGFB1	2.87	3.41	1.4E-01	9.4E-02	1.45
TGM2	1.93	2.77	2.6E-01	1.5E-01	1.79
TMEM74	11.27	12.75	4.0E-04	1.5E-04	2.78
TNF	7.43	7.86	5.8E-03	4.3E-03	1.34
TNFSF10	6.62	5.94	1.0E-02	1.6E-02	0.62
TP53	7.23	7.31	6.7E-03	6.3E-03	1.06
ULK1	7.77	8.75	4.6E-03	2.3E-03	1.97
ULK2	7.71	8.30	4.8E-03	3.2E-03	1.50
UVRAG	7.24	8.09	6.6E-03	3.7E-03	1.81
WIPI1	6.28	6.60	1.3E-02	1.0E-02	1.25

Cell line: T24 bladder cancer cells

Supplemental Table 3.
Sequence of primers used in site-directed mutagenesis (SDM), RT-qPCR and semi-quantitative RT-PCR.

Primers	Forward Sequence (5' to 3')	Reverse Sequence (5' to 3')
hCK1α-3HA R13 (siRNA-resistant CK1a)	5'- GTACTTAAATTACTGTCGTGGGCTACGCTTTG -3'	5'- CAAAGCGTAGCCCACGACAGTAATTTAAGTAC -3'
pCS2-6MT-CK1α K46A	5'- GCGAGGAAGTGGCAGTGGCGCTAGAATCTCAGAAGG -3'	5'- CCTTCTGAGATTCTAGCGCCACTGCCACTTCCTCGC -3'
FOXO3A S318A	5'- CCAATTCTAACGCCGCCACAGTCAGTGGCCGCC -3'	5'- GGCGGCCACTGACTGTGGCGGCGTTAGAATTGG -3'
FOXO3A S321A	5'- CGCCAGCACAGTCGCTGGCCGCCTGTCG -3'	5'- CGACAGGCGGCCAGCGACTGTGCTGGCG -3'
FOXO3A DM (S318A & S321A)	5'- CCAATTCTAACGCCGCCACAGTCGCTGGCCGCCTGTCG -3'	5'- CGACAGGCGGCCAGCGACTGTGGCGGCGTTAGAATTGG -3'
HPRT1	5'- CTCCGTTATGGCGACCC -3'	5'- CACCCTTTCCAAATCCTCAG -3' -3'
β-actin	5'- AAGGATTCCTATGTGGGCGACG -3'	5'- GCCTGGATAGCAACGTACATGG -3'
LC3B	5'- CGATACAAGGGTGAGAAGCAG -3'	5'- TTGAGCTGTAAGCGCCTTCTA -3'
BNIP3	5'- TCAGATTGGATATGGGATTGG -3'	5'- AGAATATGCCCCCTTTCTTCA -3'
ATG12	5'- CTGGCGACACCAAGAAAAA -3'	5'- ATGAGTCCTTGGATGGTTCG -3'
GABARAP	5'- GGAGAAAAGATCCGGAAGAAA -3'	5'- TGGCCAACAGTAAGGTCAGA -3'
FOXO3A	5'- CTGAACTCCCTACGCCAGTC -3'	5'- GAAGTGAGCAGGTCGTGGAG -3'
CSNK1A1 (CK1α)	5'- AATCTCCAGTGGGGAAGAGG -3'	5'- CCTGAGAAAGATGGGTCCTG -3'
*CSNK1D (CK1**δ**)*	5'- CCCATCGAAGTGTTGTGTAAAGG -3'	5'- GCCGCAGGTACGAGTAGTCA -3'
*CSNK1E (CK1**ε**)*	5'- AAGACGGTGCTGCTCTTGG -3'	5'- GAGGAAGTTGTCGGGCTTG -3'
DDX3X	5'- TTCTCAGATGTTTGTTGTGTGGATT -3'	5'- AAACTTGCTCAAATGCTATTGCTG -3'
ATF4	5'- TCTCCAGCGACAAGGCTAA -3'	5'- CAATCTGTCCCGGAGAAGG -3'
GADD34	5'- AGCGCCCAGAAACCCCTACTCAT -3'	5'- AGACAGCCAGGAAATGGACAGTGA -3'
GRP78	5'- GTTCTTGCCGTTCAAGGTGG -3'	5'- TGGTACAGTAACAACTGCATG -3'